Time Dependent Scattering in an Acoustic Waveguide Via Convolution Quadrature and the Dirichlet-to-Neumann Map

Li Fan, Peter Monk, and Virginia Selgas

Abstract We propose to use finite elements and BDF2 time stepping to solve the problem of computing a solution to the time dependent wave equation with a variable sound speed in an infinite sound hard pipe (waveguide). By using the Laplace transform and an appropriate Dirichlet-to-Neumann (DtN) map for the problem, we can prove that this problem can be reduced to a variational problem on a bounded domain that has a unique solution. This solution can be discretized in space using finite elements (projecting into a Fourier space on the two artificial boundaries to allow the rapid calculation of the DtN map). We discretize in time using the Convolution Quadrature (CQ) approach and in particular BDF2 time-stepping. Thanks to CQ we obtain a stable and convergent discretization of the DtN map, and hence of the fully discrete BDF2-finite element scheme without a CFL condition. We illustrate the method with some numerical results.

1 Introduction

Simulating sound propagation in pipes (also called waveguides) requires to solve the wave equation in a sound hard acoustic waveguide. In this paper we consider the use of a finite element time domain approach to the problem. We suppose that the waveguide encloses a bounded perturbation assumed to be a region in which the sound speed differs from the background speed in the rest of the waveguide. We refer to the perturbation as the scatterer. A sound wave is incident on this perturbation and produces a scattered wave that needs to be computed. For simplicity we will work in two spatial dimensions, but the algorithm we develop can be used for a true three dimensional pipe with obvious modifications.

L. Fan • P. Monk
Department of Mathematical Sciences, University of Delaware, Newark, DE 19716, USA
e-mail: fanli0218@gmail.com; monk@udel.edu

V. Selgas (✉)
Departamento de Matemáticas, Universidad de Oviedo, EPIG, 33203 Gijón, Spain
e-mail: selgasvirginia@uniovi.es

F. Ortegón Gallego et al. (eds.), *Trends in Differential Equations and Applications*,
SEMA SIMAI Springer Series 8, DOI 10.1007/978-3-319-32013-7_18

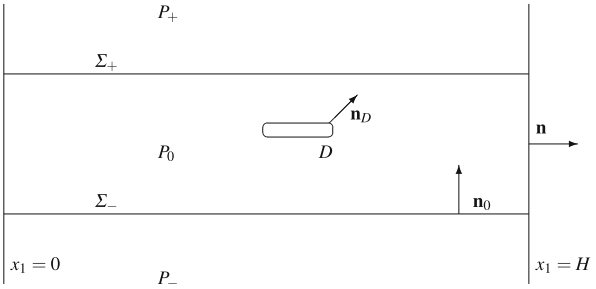

Fig. 1 Cartoon of the main geometric elements used in our analysis. Finite elements are used in the domain P_0 which includes the scatterer D. The artificial boundaries are Σ_- and Σ_+

Let us consider a waveguide $P = (0, H) \times \mathbb{R}$, containing an obstacle D which is assumed to be bounded and have a Lipschitz continuous boundary. Denote by $\mathbf{n}$ the unit outward normal on ∂P, i.e. $\mathbf{n} = (-1, 0)$ on $x_1 = 0$ and the opposite on $x_1 = H$. Similarly, we use the notation $\mathbf{n}_D$ for the unit outward normal on ∂D. Figure 1 shows a graphic of the computational domain.

The refractive index $\mathrm{n}(\mathbf{x})$ is assumed to be real and frequency independent, and such that $\mathrm{n}(\mathbf{x}) = 1$ if $\mathbf{x} \in P \setminus \overline{D}$ and $\mathrm{n}(\mathbf{x}) \neq 1$ if $\mathbf{x} \in D$. Later in the paper we will comment on impenetrable scatterers and frequency dependent coefficients. The speed of sound in the background waveguide outside D is a constant c_0.

We suppose that a given incident field u_{inc} hits the scatterer. The incident field is a bounded smooth solution of the background wave equation so that it satisfies the wave equation in the free waveguide:

$$\begin{aligned} \frac{1}{c_0^2}\partial_{tt}^2 u_{inc} &= \Delta u_{inc} \quad \text{in } \mathbb{R} \times P\,, \\ \partial_{\mathbf{n}} u_{inc} &= 0 \quad \text{on } \mathbb{R} \times \partial P\,, \end{aligned}$$

where ∂_{tt}^2 denotes the second time derivative, and $\partial_{\mathbf{n}}$ denotes the normal derivative. The boundary condition models a sound hard wall. In the sequel we assume that the incident field u_{inc} does not hit the scatterer D before $t = 0$, that is,

$$u_{inc} = \partial_t u_{inc} = \partial_{tt}^2 u_{inc} = 0 \quad \text{in } \overline{D},\ \text{for } t \leq 0\,. \tag{1}$$

In the time domain, the wave equation and boundary conditions for the total wave u and the scatterer field u_{sc} are

$$\begin{aligned} \frac{\mathrm{n}^2}{c_0^2}\partial_{tt}^2 u &= \Delta u \quad \text{in } P,\ \text{for } t > 0\,, \\ u &= u_{inc} + u_{sc} \quad \text{in } P,\ \text{for } t > 0\,, \\ \partial_{\mathbf{n}} u &= 0 \quad \text{on } \partial P,\ \text{for } t > 0\,, \\ u &= 0 \quad \text{in } P,\ \text{at } t = 0, \\ \partial_t u &= 0 \quad \text{in } P,\ \text{at } t = 0. \end{aligned} \tag{2}$$

Here n is understood to be a function of positions $\mathbf{x}$. There is no need for a condition at infinity because u_{sc} propagates with finite velocity and so for any $t > 0$ there is a distance $M(t)$ such that $u_{sc}(t, \mathbf{x}) = 0$ for any $\mathbf{x} = (x_1, x_2)$ with $x_1 \in (0, H)$, $|x_2| > M(t)$. Our problem is to approximate u (or equivalently u_{sc}) and we shall use finite elements in space because they can approximate general boundaries of the scatterer easily.

To use finite elements we introduce a computational domain $P_0 := (0, H) \times (0, L)$ for $L > 0$ big enough to enclose the scatterer, that is, such that $\overline{D} \subset P_0$ (see Fig. 1). Then we can cover P_0 with finite elements (in our case using triangles). The only obstacle to a standard finite element approach in space is the need for a special artificial boundary condition at $x_2 = 0$ and $x_2 = L$ that takes care of the infinite waveguide on either side of P_0. This can be constructed using the Perfectly Matched Layer (PML) (see [9]); in fact, provided the PML is chosen to handle both traveling and evanescent modes in the solution this can be very successful. However the PML is difficult to analyze and requires an informed choice of the PML parameters so instead we propose to use a time domain Dirichlet-to-Neumann (DtN) map on the artificial interfaces $x_2 = 0$ and $x_2 = L$ following the approach of [6]. With this approach we need to store the solution on the artificial boundaries for all time steps, but, at least at low frequencies and in two dimensions this is not a crushing problem since only a few modes need to be stored for each time step.

We propose to use implicit time stepping to take care of possible refined meshes in some regions of the simulations, as well as to allow for changes in refractive index from place to place (this would change the CFL of an explicit scheme from place to place). In particular we shall use the Laplace transform to analyze the truncated problem (cf. [1, 7]) and convolution quadrature (cf. [10]) to prove that a family of time stepping schemes including Backward Differentiation Formula 2 (BDF2) give rise to stable and convergent time stepping method. An added bonus is that, at least before spatial discretization, the method shows how to construct perfect discrete DtN maps matched to the time stepping scheme. An alternative approach using more standard time stepping and integral equations on the interfaces might be constructed along the line of [3], but we do not pursue that here.

The paper proceeds as follows. In the next section we give details of how to reduce the problem to a family of Laplace domain equations posed on the computational domain P_0. Then in Sect. 3 we summarize the analysis of the Laplace domain problems, and then relate these back to a fully discrete time stepping scheme using convolution quadrature. The fully discrete scheme is shown to be optimally convergent. Then in Sect. 4 we provide a few numerical results from our method implemented using the multi-frequency approach of Banjai and Sauter proposed in [2].

2 Reduction to a Bounded Domain

It is convenient to perform the initial analysis using the scattered field $u_{sc} = u - u_{inc}$ which satisfies

$$\frac{\mathrm{n}^2}{c_0^2}\partial_{tt}^2 u_{sc} = \Delta u_{sc} + F \quad \text{in } P, \text{ for } t > 0\,,$$
$$\partial_{\mathbf{n}} u_{sc} = 0 \quad \text{on } \partial P, \text{ for } t > 0. \tag{3}$$

Above, we have set

$$F = \frac{1}{c_0^2}(1 - \mathrm{n}^2(\mathbf{x}))\partial_{tt}^2 u_{inc}\,.$$

Notice that $F = 0$ outside D, for any $t \in \mathbb{R}$, since $\mathrm{n}(\mathbf{x}) = 1$ there. Furthermore, $F = 0$ in the whole P_0 for any $t \leq 0$ according to (1). On the other hand, (1) also suggests that the scattered field is causal and, hence, we impose the initial conditions

$$u_{sc} = \partial_t u_{sc} = 0 \quad \text{in } P, \text{ at } t = 0.$$

In order to analyze (3), we transform it to the Laplace domain. More precisely, for any smooth and causal function $f(t)$, the Laplace transform we use is defined as

$$\mathscr{L}[f](s) = \int_0^\infty f(t)\exp(-st)\,dt \quad \text{for } s \in \mathbb{C}_\sigma\,,$$

where $\mathbb{C}_\sigma = \{s;\ s = \eta - i\omega \text{ with } \eta > \sigma\eta, \omega \in \mathbb{R}, \eta > \sigma,\ \omega \in \mathbb{R}\}$ for a fixed positive $\sigma \in \mathbb{R}$. Then, working formally with Eq. (3), we have that the Laplace transform of the scattered field, $\hat{u}_{sc} = \mathscr{L}[u_{sc}](s)$, solves

$$\frac{s^2\mathrm{n}^2}{c_0^2}\hat{u}_{sc} = \Delta\hat{u}_{sc} + \hat{F} \quad \text{in } P\,, \tag{4}$$
$$\partial_{\mathbf{n}}\hat{u}_{sc} = 0 \quad \text{on } \partial P\,. \tag{5}$$

Above, $\hat{F}$ stands for the Laplace transform of F; let us recall that $\hat{F} = 0$ in $P \setminus \overline{D}$.

As already mentioned, we make use of a bounded section of the pipe $P_0 = (0, H) \times (0, L)$ containing the scatterer D in its interior (see Fig. 1). Then, adopting the usual Galerkin strategy, the problem in P_0 consists in finding $\hat{u}_{sc} \in H^1(P_0)$ such that, for any $v \in H^1(P_0)$,

$$\int_{P_0} \frac{\mathrm{n}^2}{c_0^2}s^2\hat{u}_{sc}\,\overline{v} + \int_{P_0}\nabla\hat{u}_{sc}\cdot\nabla\overline{v} - \int_{\Sigma_+}\partial_{\mathbf{n}_0}\hat{u}_{sc}\,\overline{v} + \int_{\Sigma_-}\partial_{\mathbf{n}_0}\hat{u}_{sc}\,\overline{v} = \int_{P_0}\hat{F}\,\overline{v}\,, \tag{6}$$

where the unit vector $\mathbf{n}_0 = (0,1)$ is normal to the artificial boundaries $\Sigma_- = (0,H)\times\{0\}$ and $\Sigma_+ = (0,H)\times\{L\}$.

In order to deal with the integrals on $\Sigma_\pm$, we next define the DtN maps $\hat{T}^s_\pm(\hat{u}_{sc}) = \pm\partial_{\mathbf{n}_0}\hat{u}_{sc}$ on $\Sigma_\pm$. Working in the remaining parts of the pipe $P\setminus\overline{P_0}$, where we have a homogeneous wave equation, we may obtain explicit expressions of the DtN maps.

More precisely, let us start by considering $P_- = (0,H)\times(-\infty,0)$. Then $\hat{u}_{sc}\in H^1(P_-)$ satisfies

$$\frac{s^2}{c_0^2}\hat{u}_{sc} = \Delta\hat{u}_{sc} \quad \text{in } P_-\,, \tag{7}$$

$$\partial_{\mathbf{n}}\hat{u}_{sc} = 0 \quad \text{on } \partial P_-\setminus\Sigma_-\,. \tag{8}$$

Taking advantage of Eq. (8), we write the scattered field in P_- as

$$\hat{u}_{sc}(x_1,x_2) = \sum_{m=0}^{\infty} u_m(x_2)\,\cos\Big(\frac{m\pi x_1}{H}\Big) \quad \text{in } P_-\,, \tag{9}$$

where each $u_m(x_2)$ is bounded for $x_2\to-\infty$. Then, Eq. (7) means that

$$-(u_m)'' + \frac{m^2\pi^2}{H^2}u_m + \frac{s^2}{c_0^2}u_m = 0 \quad \text{for } x_2<0\,. \tag{10}$$

Also notice that $u_m(0) = u_{m,0}$, where $\{u_{m,0}\}_{m=0}^{\infty}$ are the complex Fourier expansion coefficients of $\hat{u}_{sc}$ on Σ_-:

$$\hat{u}_{sc} = \sum_{m=0}^{\infty} u_{m,0}\,\cos\Big(\frac{m\pi x_1}{H}\Big) \quad \text{on } \Sigma_-\,.$$

In consequence, denoting

$$\kappa_m \equiv \kappa_m(s) = \frac{s}{c_0}\sqrt{1+\frac{m^2\pi^2}{H^2}\,\frac{c_0^2}{s^2}}\,, \tag{11}$$

and choosing $\Re(\kappa_m)>0$ we have

$$\hat{u}_{sc}(x_1,x_2) = \sum_{m=0}^{\infty} u_{m,0}\,\cos\Big(\frac{m\pi x_1}{H}\Big)\,\exp(\kappa_m x_2) \quad \text{in } P_-\,. \tag{12}$$

In particular, it follows that

$$\partial_{\mathbf{n}_0}\hat{u}_{sc} = \partial_{x_2}\hat{u}_{sc} = \sum_{m=0}^{\infty}\kappa_m\,u_{m,0}\,\cos\Big(\frac{m\pi x_1}{H}\Big) \quad \text{on } \Sigma_-\,. \tag{13}$$

Summing up, we have the following explicit expression of the DtN map on Σ_-:

$$\hat{T}^s_- \xi = -\sum_{m=0}^{\infty} \kappa_m(s)\, \xi_m \cos\left(\frac{m\pi x_1}{H}\right) \quad \text{on } \Sigma_-\,, \tag{14}$$

for any ξ whose Fourier expansion on Σ_- is

$$\xi = \sum_{m=0}^{\infty} \xi_m \cos\left(\frac{m\pi x_1}{H}\right), \tag{15}$$

where ξ_m $(m = 0, \ldots, \infty)$ are the complex expansion coefficients.

Similarly, we can work in P_+ to obtain an explicit expression of $\hat{T}^s_+$ on Σ_+. We now make use of the DtN maps to rewrite the variational formulation (6) of the model problem in the Laplace domain as follows: Find $\hat{u}_{sc} \in H^1(P_0)$ such that, for any $v \in H^1(P_0)$,

$$\int_{P_0} \frac{\mathrm{n}^2}{c_0^2} s^2 \hat{u}_{sc}\, \overline{v} + \int_{P_0} \nabla \hat{u}_{sc} \cdot \nabla \overline{v} - \int_{\Sigma_+} \hat{T}^s_+ \hat{u}_{sc}\, \overline{v} - \int_{\Sigma_-} \hat{T}^s_- \hat{u}_{sc}\, \overline{v} = \int_{P_0} \hat{F}\, \overline{v}\,. \tag{16}$$

3 Convergence Analysis

The analysis of existence, uniqueness and finite element convergence for the variational problem in the Laplace domain (16) follows the general steps of the analysis of the periodic grating problem in [6]. According to this, we only make an outline of the most important results of such analysis. To this end, we start introducing the following s-dependent norm on $H^1(P_0)$:

$$\|v\|_{s,H^1(P_0)} = \left(\int_{P_0} \left(\frac{|s|^2}{c_0^2}|v|^2 + |\nabla v|^2\right) d\mathbf{x}\right)^{1/2} \quad \text{for } v \in H^1(P_0)\,.$$

For each $r \in [0, 1]$, we define the following s-dependent norm on $H^r(\Sigma_\pm)$:

$$\|\xi\|_{s,H^r(\Sigma_\pm)} = \left(\sum_{m=0}^{+\infty} \left(\frac{|s|^2}{c_0^2} + \frac{m^2\pi^2}{H^2}\right)^r |\xi_m|^2\right)^{1/2},$$

for any $\xi \in H^r(\Sigma_\pm)$ written by means of its Fourier expansion (15). We also define the associated s-dependent norm on $H^{-r}(\Sigma_\pm)$ by duality.

Notice that the s-dependent $H^1(P_0)$ norm corresponds to a weighted energy for the field after inverse Laplace transforming back to the time domain. Besides, the s-dependent boundary norm on $H^r(\Sigma_\pm)$ is chosen so that both the trace of functions

in $H^1(P_0)$ and the DtN maps can be estimated by appropriate norm bounds with explicit s-independence, as we detail in the following subsection.

3.1 Well-Posedness of the Variational Problem in the Laplace Domain

Following directly the argument in [6, Lemma 2.1] we can show the following bound of the trace operator $\gamma_{\Sigma_\pm} : H^1(P_0) \to H^{1/2}(\Sigma_\pm)$ in terms of weighted norms:

$$\|\gamma_{\Sigma_\pm} v\|_{s,H^{1/2}(\Sigma_\pm)} \leq C_1 \, \|v\|_{s,H^1(P_0)} \quad \text{for } v \in H^1(P_0)\,,$$

where $C_1 = 2\sqrt{\frac{2\,c_0}{LH\sigma}}$.

Moreover, using the Fourier definition of the DtN operator (14) and reasoning as in the proof of [6, Lemma 2.2], we deduce the following bound of the DtN operators $\hat{T}^s_\pm : H^{1/2}(\Sigma_\pm) \to H^{-1/2}(\Sigma_\pm)$ in terms of weighted norms:

$$\|\hat{T}^s_\pm \xi\|_{s,H^{-1/2}(\Sigma_\pm)} \leq C \|\xi\|_{s,H^{1/2}(\Sigma_\pm)} \quad \text{for } \xi \in H^{1/2}(\Sigma_\pm)\,,$$

where C is independent of s.

We can now analyze the variational formulation of the Laplace domain problem on P_0 applying the Lax-Milgram Lemma. To this end, we define the s-dependent sesquilinear form $a^s : H^1(P_0) \times H^1(P_0) \to \mathbb{C}$ associated to the variational formulation (16), given by

$$a^s(w,v) := \int_{P_0} \frac{\mathrm{n}^2}{c_0^2} s^2 \, w\, \overline{v} + \int_{P_0} \nabla w \cdot \nabla \overline{v} - \int_{\Sigma_+} \hat{T}^s_+ w\, \overline{v} - \int_{\Sigma_-} \hat{T}^s_- w\, \overline{v}\,.$$

Let us emphasize the following properties of the sesquilinear form $a^s(\cdot,\cdot)$ in terms of $s \in \mathbb{C}_\sigma$:

- By using the definition of the s-dependent $H^1(P_0)$ norm, and the bounds on the trace operator and the DtN maps, we have the following continuity bound:

$$|a^s(w,v)| \leq C_2 \, \|w\|_{s,H^1(P_0)} \, \|v\|_{s,H^1(P_0)}\,, \tag{17}$$

  where $C_2 = \max\{1, \|\mathrm{n}^2\|_{L^\infty(P_0)}\} + 8\frac{c_0}{LH\sigma}$.
- Using Bamberger and HaDuong's technique [1] as in the proof of [6, Lemma 3.1], we have the following coercivity bound in terms of s-dependent norms

$$\Re(a^s(v, sv)) \geq \sigma \inf_{\mathbf{x}\in P_0} \mathrm{n}^2(\mathbf{x}) \, \|v\|^2_{s,H^1(P_0)}\,. \tag{18}$$

Notice that the estimates (17) and (18) make clear their dependence on both $s \in \mathbb{C}_\sigma$ and $w, v \in H^1(P_0)$. In particular, we can apply the Lax–Milgram theorem to guarantee the well-posedness of problem (16); moreover, we have the following bound on its unique solution:

$$\|\hat{u}_{sc}\|_{s,H^1(P_0)} \leq \frac{C}{\sigma} \|\hat{F}\|_{L^2(P_0)} ,$$

where C is independent of s, $\hat{u}_{sc}$ and $\hat{F}$.

3.2 Spatial Discretization of the Problem in the Laplace Domain

Discretization of $H^1(P_0)$ is by standard finite elements. More precisely, we consider a regular mesh family $\mathscr{T}_h$, $h > 0$, of P_0 consisting of triangles K of maximum diameter h and which can be mapped from the reference triangle element $\hat{K}$ using an affine mapping $m_K : \hat{K} \to K$. Then we define the finite element space $\mathbb{S}_h$ of continuous finite elements on $\mathscr{T}_h$. In particular

$$\mathbb{S}_h := \{f \in \mathscr{C}^0(P_0); f|_K = \hat{f} \circ m_K \text{ for some } \hat{f} \in \mathbb{P}_q \ \forall K \in \mathscr{T}_h\} ,$$

where $\mathbb{P}_q$ denotes the set of complex valued polynomials of total degree at most q.

The only remaining difficulty in discretizing the variational problem by means of the approximation space $\mathbb{S}_h$ is that we need to apply the DtN operators to traces of finite element functions. This could be done using an integral equation on $\Sigma_\pm$ as in [3], but for the simple geometry here we can truncate the Fourier expansions involved in the explicit expression of the DtN maps. This may be done efficiently by means of a trigonometric basis of $H^{1/2}(\Sigma_\pm)$, which is a common strategy in the frequency domain. More precisely, let us introduce the finite-dimensional space

$$\mathscr{P}_N := \text{span}\left\{\cos\left(\frac{m\pi x_1}{H}\right); m = 0, 1, \ldots, N\right\} ,$$

as well as the $L^2(\Sigma_\pm)$ orthogonal projections $p_{N,\pm} : L^2(\Sigma_\pm) \to \mathscr{P}_N$. We then approximate the operators $\hat{T}^s_\pm$ by means of $\hat{T}^s_{N,\pm} = \hat{T}^s_\pm \circ p_{N,\pm}$, and the s-dependent sesquilinear forms $a^s : H^1(P_0) \times H^1(P_0) \to \mathbb{C}$ by

$$a^s_{h,N}(w, v) := \int_{P_0} \frac{\mathrm{n}^2}{c_0^2} s^2 \, w \, \overline{v} + \int_{P_0} \nabla w \cdot \nabla \overline{v} - \int_{\Sigma_+} \left(\hat{T}^s_{N,+} w\right) p_{N,+} \overline{v}$$
$$- \int_{\Sigma_-} \left(\hat{T}^s_{N,-} w\right) p_{N,-} \overline{v} .$$

With this approach, the discrete counterpart of problem (16) consists of finding $\hat{u}_{sc,h,N} \in \mathbb{S}_h$ such that, for any $v \in \mathbb{S}_h$,

$$a^s_{h,N}(\hat{u}_{sc,h,N}, v) = \int_{P_0} \hat{F}\,\overline{v}\,. \tag{19}$$

Reasoning as at continuous level, we can see that the discrete sesquilinear form $a^s_{h,N}(\cdot,\cdot)$ is bounded and coercive in terms of s-dependent norms, here again with the same dependence on $s \in \mathbb{C}_\sigma$ and σ as in the continuous case. Indeed, properties (17) and (18) remain valid if we replace the sesquilinear form $a^s : H^1(P_0)\times H^1(P_0) \to \mathbb{C}$ by its discrete counterpart $a^s_{h,N} : H^1(P_0) \times H^1(P_0) \to \mathbb{C}$. In particular, this allows us to reason just as we did before to guarantee the existence of a unique solution of the discrete problem (19), $\hat{u}_{sc,h,N} \in \mathbb{S}_h$, and deduce the following bound:

$$\|\hat{u}_{sc,h,N}\|_{s,H^1(P_0)} \leq \frac{C}{\sigma}\,\|\hat{F}\|_{L^2(P_0)}\,.$$

This result is analogous to [6, Theorem 3.4].

We can then prove an error estimate based on Strang's second lemma in which we keep track of the dependence on the parameter $s \in \mathbb{C}_\sigma$. The analysis is similar to [6, Theorem 3.5]:

$$\begin{aligned}\|\hat{u}_{sc} - \hat{u}_{sc,h,N}\|_{s,H^1(P_0)} \leq \frac{|s|}{\sigma}\Big(&\Big(\frac{C_2}{\inf_{\mathbf{x}\in P_0} \mathrm{n}^2(\mathbf{x})} + 1\Big)\,\|\hat{u}_{sc} - \hat{w}_h\|_{s,H^1(P_0)} \\ &+C_1\,\|\gamma_{\Sigma_+}\hat{u}_{sc} - p_{N,+}\gamma_{\Sigma_+}\hat{u}_{sc}\|_{s,H^{1/2}(\Sigma_+)} \\ &+C_1\,\|\gamma_{\Sigma_-}\hat{u}_{sc} - p_{N,-}\gamma_{\Sigma_-}\hat{u}_{sc}\|_{s,H^{1/2}(\Sigma_-)}\Big)\,,\end{aligned}$$

where $\hat{w}_h \in \mathbb{S}_h$ and C_1 and C_2 are the s-independent constants previously introduced (see (17) and (18)).

By taking the inverse Laplace transform of the above estimate, we can then derive an error estimate for the semi-discrete approximation $u_{sc,h,N}$ of u_{sc} (i.e. only discretizing in space). More precisely, following the approach of [10], let $T > 0$ denote the final time for the solution and set

$$H^r_0((0,T);X) = \{u \in H^r((-\infty,T);X)\ ;\ u(t,\cdot) = 0 \text{ for } t < 0\}\,, \tag{20}$$

where X stands for any Hilbert space. We then have the following theorem.

Theorem 1 *Assume that $\hat{F} \in L^2(\Omega)$, $s = \sigma - i\omega$ with $\sigma > \sigma_0$ and $n^2 > \delta$, for some constants $\sigma_0, \delta > 0$. Then there exists a unique solution $\hat{u}^s_{sc,h,N} \in \mathbb{S}_h$ to (19) and furthermore there is a constant C such that, for any $t \in (0,T)$ and*

$v_h \in H_0^2((0,T);\mathbb{S}_h)$,

$$\begin{aligned}\|u_{sc,h,N}(t) - u_{sc}(t)\|_{H^1(P_0)} \le C \Big(& \|u_{sc} - v_h\|_{H_0^2((0,T);H^1(P_0))} \\ & + \|p_{N,+}u_{sc} - u_{sc}\|_{H_0^2((0,T);H^{1/2}(\Sigma_+))} \\ & + \|p_{N,-}u_{sc} - u_{sc}\|_{H_0^2((0,T);H^{1/2}(\Sigma_-))} \Big). \end{aligned} \quad (21)$$

Here C depends on T but is independent of u_{sc} and t, and of the discretization parameters h and N.

3.3 Discretization in Time

Following the Convolution Quadrature (CQ) approach proposed in [10], to discretize in space and time we can use the discrete Laplace transform. To do this we need to choose a suitable time discretization. Let Δt denote the time step $\Delta t = T/N_t$ where N_t is the number of time steps, and let $t_n = n\Delta t$. As usual for CQ, a good choice of multistep method is BDF2 which approximates the solution $y(t)$ of $y' = f(t,y)$ using the difference equation

$$\frac{3}{2}y_{n+2} - 2y_{n+1} + \frac{1}{2}y_n = \Delta t f(t_{n+2}, y_{n+2}) \quad \text{for } n = -1, 0, 1, \ldots,$$

where $y_n = 0$ for $n \le 0$. The generating polynomial for this method is

$$\gamma(\zeta) = \frac{3}{2} - 2\zeta + \frac{1}{2}\zeta^2 \quad \text{for } \zeta \in \mathbb{C}.$$

The discrete time Laplace transform of the solution we wish to find is denoted $\hat{u}^{\Delta t}_{sc,h,N} \in \mathbb{S}_h$ and satisfies the Laplace domain variational problem with s replaced by $\gamma(\zeta)/\Delta t$:

$$a^{\gamma(\zeta)/\Delta t}(\hat{u}^{\Delta t}_{sc,h,N}, v_h) = \int_{P_0} \hat{F}|_{s=\gamma(\zeta)/\Delta t}\, \overline{v_h} \quad \text{for all } v_h \in \mathbb{S}_h, \quad (22)$$

where this equation holds for all $\zeta \in \mathbb{C}$ with $|\zeta| < 1$.

Taking the inverse discrete Laplace transform we obtain a fully discrete time stepping problem that determines $u^{\Delta t,n}_{sc,h,N} \in \mathbb{S}_h$ for $n = 0, 1, \ldots$. In particular, as in [6] we introduce a new variable

$$\hat{z}^{\Delta t}_{h,N} = \frac{\gamma(\zeta)}{\Delta t}\, \hat{u}^{\Delta t}_{sc,h,N}, \tag{23}$$

so that (22) can be rewritten as finding $\hat{u}^{\Delta t}_{sc,h,N} \in \mathbb{S}_h$ such that

$$\int_{P_0} \frac{\mathrm{n}^2}{c_0^2}\, \frac{\gamma(\zeta)}{\Delta t}\, \hat{z}^{\Delta t}_{h,N}\, \overline{v_h} + \int_{P_0} \nabla \hat{u}^{\Delta t}_{sc,h,N} \cdot \nabla \overline{v_h} - \int_{\Sigma_+} \hat{T}_+^{\gamma(\zeta)/\Delta t}(p_N \hat{u}^{\Delta t}_{sc,h,N})\, \overline{v_h}$$
$$- \int_{\Sigma_-} \hat{T}_-^{\gamma(\zeta)/\Delta t}(p_N \hat{u}^{\Delta t}_{sc,h,N})\, \overline{v_h} = \int_{P_0} \hat{F}|_{s=\gamma(\zeta)/\Delta t} \overline{v}_h \quad \text{for all } v_h \in \mathbb{S}_h\,. \tag{24}$$

Introducing the z-transform of the discrete time solution as

$$\hat{u}^{\Delta t}_{sc,h,N} = \sum_{m=0}^{\infty} u^{\Delta t,m}_{sc,h,N}\, \zeta^m, \qquad \hat{z}^{\Delta t}_{h,N} = \sum_{m=0}^{\infty} z^{\Delta t,m}_{h,N}\, \zeta^m,$$

and equating terms in ζ in (23) shows that the standard BDF2 equation is satisfied

$$\frac{1}{\Delta t}\left(\frac{3}{2} u^{\Delta t,m}_{sc,h,N} - 2u^{\Delta t,m-1}_{sc,h,N} + \frac{1}{2} u^{\Delta t,m-2}_{sc,h,N}\right) = z^{\Delta t,m}_{sc,h,N}$$

for each $m \geq 0$ where $u^{\Delta t,p}_{sc,h,N} = 0$ if $p \leq 0$.

To analyze (24) suppose that we have a finite Fourier series $w = \sum_{m=0}^{N} w_m \cos(m\pi x_1/H)$. Then from (14) we see that

$$\hat{T}^{\gamma(\zeta)/\Delta t} w = -\sum_{m=0}^{N} \kappa_m\left(\frac{\gamma(\zeta)}{\Delta t}\right) w_m \cos\left(\frac{m\pi x_1}{H}\right),$$

where $\kappa_m(s)$ is given by (11). The same expansion holds for $\hat{T}_+^{\gamma(\zeta)/\Delta t}$. Expanding $\kappa_m(\gamma(\zeta)/\Delta t)$ in terms of ζ gives

$$\kappa_m\left(\frac{\gamma(\zeta)}{\Delta t}\right) = \sum_{j=0}^{\infty} \kappa^{\Delta t}_{m,j} \zeta^j,$$

for some coefficients $\kappa^{\Delta t}_{m,j}$ when $|\zeta| < 1$. These coefficients can be computed exactly for small values of j and in general computed numerically using a discrete

approximation to the Cauchy integral formula as in [4, 6]. For example

$$\kappa_{m,0}^{\Delta t} = \frac{\sqrt{4\pi^2 c_0^2 (\Delta t)^2 m^2 + 9H^2}}{2\Delta t\, c_0 H},$$

$$\kappa_{m,1}^{\Delta t} = -6\,\frac{H}{\Delta t\, c_0 \sqrt{4\pi^2 c_0^2 (\Delta t)^2 m^2 + 9H^2}},$$

$$\kappa_{m,2}^{\Delta t} = \frac{\left(44\pi^2 c_0^2 (\Delta t)^2 m^2 + 27H^2\right) H}{2\Delta t\, c \left(4\pi^2 c_0^2 (\Delta t)^2 m^2 + 9H^2\right)^{3/2}},$$

and so on. Now define

$$\tilde{T}_{\pm}^{(j)} w = -\sum_{m=0}^{N} \kappa_{m,j}^{\Delta t}\, w_m\, \cos(\frac{m\pi x_1}{H})\,.$$

Equating powers of ζ in (24) gives

$$\int_{P_0} \frac{\mathrm{n}^2}{c_0^2 \Delta t}\left(\frac{3}{2} z_{sc,h,N}^{\Delta t,m} - 2 z_{sc,h,N}^{\Delta t,m-1} + \frac{1}{2} z_{sc,h,N}^{\Delta t,m-2}\right)\overline{v_h} + \int_{P_0} \nabla u_{sc,h,N}^{\Delta t,m} \cdot \nabla \overline{v_h}$$
$$- \sum_{j=0}^{m} \int_{\Sigma_+} \tilde{T}_{+}^{(j)} (p_N u_{sc,h,N}^{\Delta t,m-j})\,\overline{v_h} - \sum_{j=0}^{m} \int_{\Sigma_-} \tilde{T}_{-}^{(j)} (p_N u_{sc,h,N}^{\Delta t,m-j})\,\overline{v_h} = \int_{P_0} \hat{F}^{\Delta t,m} \overline{v}_h\,, \tag{25}$$

for all $v_h \in \mathbb{S}_h$.

We see that inside P_0 the method corresponds to using BDF2 and finite elements for the wave equation. On the artificial boundaries $\Sigma_\pm$ the method provides a discrete approximation to the DtN map that uses a discrete convolution at each time step. In particular, at time step m this requires access to the $N+1$ Fourier coefficients of $u_{sc,h,N}^{\Delta t,j}$ for $j = 0,\ldots,m$ on the two artificial boundaries. Thus storage requirements grow with time, but for pipes at low frequency there are few propagating modes and so N is not large (besides the propagating modes, some evanescent modes also need to be stored depending how far the artificial boundary is away from the scatterer).

At the expense of more notation, we can now eliminate $z_{sc,h,N}^{\Delta t,m}$ from the difference equation to obtain the discretization of a second order in time problem for u_{sc} alone.

Following Lubich's strategy [10] as in [6] we can prove the following fully discrete error estimate where $W_0^4((0,T);L^1(P_0))$ is defined analogously to $H_0^r((0,T);X)$ in (20):

Theorem 2 *Suppose we use BDF2 to discretize in time, and regular finite elements to discretize in space. In addition, suppose* $F \in W_0^4((0,T);L^1(P_0))$. *Then the time*

discrete finite element solution $u^{\Delta t,n}_{sc,h,N}$ is well defined for each time step $n = 0, 1, \ldots$ and satisfies the error estimate

$$\|u^{\Delta t,n}_{sc,h,N} - u_{sc}(t_n)\|_{H^1(P_0)} \leq C \left((\Delta t)^2 \int_0^T \int_{P_0} \left|\partial_t^4 F\right| + \|u_{sc} - v_h\|_{H^2_0((0,T);H^1(P_0))} \right.$$
$$\left. + \|p_{N,-}u_{sc} - u_{sc}\|_{H^2_0((0,T);H^{1/2}(\Sigma_-))} + \|p_{N,+}u_{sc} - u_{sc}\|_{H^2_0((0,T);H^{1/2}(\Sigma_+))} \right)$$

for any $v_h \in H^2_0((0,T);\mathbb{S}_h)$. Here the constant C depends on T and Σ_+, but is independent of u_{sc} and v_h, and the discretization parameters h, N and Δt .

The theory we have outlined extends to impenetrable (sound hard or sound soft scatterers with little change). For frequency dependent refractive indices, the Laplace domain results can be proved under suitable conditions on the behavior of the refractive index in the Laplace domain (see for example [5]).

4 Numerical Results

Although the analysis of problem (16) and its discretization are written in terms of the Laplace transform of the scattered field, in practice we approximate the total field $u = u_{sc} + u_{inc}$. This avoids performing area integrals for F. Assuming the source of the incident wave is in the section of the pipe P_-, in the Laplace domain and after discretization in space, we seek $\hat{u}_{h,N} \in \mathbb{S}_h$ which is the unique solution of

$$a^s_{h,N}(\hat{u}_{h,N}, v_h) = \int_{\Sigma_-} \partial_{\mathbf{n}_0} \hat{u}_{inc}\, \overline{v_h} - \int_{\Sigma_-} \hat{T}^s_- \hat{u}_{inc}\, \overline{v_h}\,, \tag{26}$$

for any $v_h \in \mathbb{S}_h$. Notice that there is no need for a boundary condition on Σ_+ since the total field is outgoing there.

To deal with problem (26), in practice we approximate $\hat{T}^s_- \hat{u}_{inc}$ by $\hat{T}^s_{N,-}\hat{u}_{inc}$. Above we have shown how the Laplace domain problem can be converted into a time stepping problem using CQ as in [10]. Here, to demonstrate the method, we instead use the discrete Laplace transform approach from [4]. Suppose the final time of integration is T and we wish to take N_t timesteps. In Banjai and Sauter's approach (26) is solved for N_t choices of s chosen depending on the time-stepping method used (in fact fewer problems need to be solved in practice). An inverse discrete transform then gives the time dependent solution. We use the parameter choices from [4] even though the theory in that paper is for an integral equation based approach.

4.1 Convergence Rate

To obtain a simple exact solution we can consider an empty pipe. In this case the total field is simply given by the incident field, and the code must propagate the incident field through the finite element domain. We choose the computational domain to be $P_0 = (0, 0.6) \times (0, 1)$ with Σ_- at $x_2 = 0$ and Σ_+ at $x_2 = 1$, and the width of the pipe $H = 0.6$. The final time is $T = 6$ by which time the wave has almost left the computational domain. The incident field is a plane wave $u_{inc} = f(t - x_1/c)$ where $c = 1$ and

$$f(\tau) = \cos(2\pi(\tau - H/c)) \exp(-1/(2\sigma^2)(\tau - L/c - t_p)^2)$$

where $t_p = 3$, $\sigma = 6/(2\pi\ b_w)$, and $b_w = 1.71$ denotes the bandwidth of the incident field; notice that the center frequency is 1. The parameters are chosen so that f is approximately zero in P_0 at $t = 0$. We choose a fixed spatial mesh shown in Fig. 2 (left panel) where the mesh size is $h \approx 0.016$, and use piecewise linear finite elements in space (using the FreeFem++ to implement the algorithm [8]) and BDF2 in time. Although only one mode is needed for the DtN maps in this case, we choose $N = 7$ for the Fourier spaces on Σ_- and Σ_+.

For simplicity we report the discrete maximum norm error at the nodes in the mesh as a function of N_t in the right hand panel of Fig. 2. The convergence rate is consistent with $O(N_t^{-2})$ convergence for at least part of the convergence history. We have no explanation for the increased rate at $N_t = 1024$. In any case the numerical results show that we can obtain accurate and convergent solutions over a wide range of time step sizes. Indeed, the coarsest time step is $\Delta t \approx 0.09$ and the finest time step is $\Delta t \approx 0.006$, and stability is seen across this range of time steps.

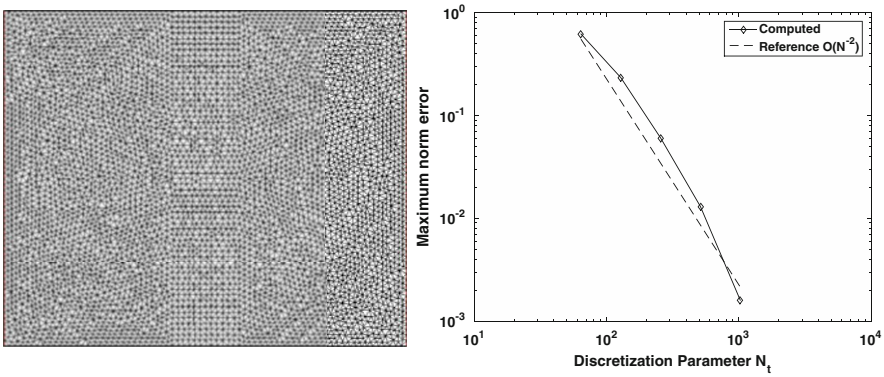

Fig. 2 Using the fixed spatial mesh shown in the *left hand* panel, we show the discrete maximum norm error at the spatial nodes as a function of the number of time steps in the *right hand panel*. We have predicted N_t^{-2} error in the $H^1(P_0)$ norm and see somewhat better than this rate at finer temporal discretization

4.2 Scattering from a Penetrable and Impenetrable Obstacles

Our next examples illustrate the flexibility of this approach since the finite element method can handle different boundary conditions and possible inhomogeneity of the scatterer. We start with a penetrable scatterer as analyzed in this paper. We choose $\mathrm{n}(\mathbf{x}) = 1$ in the pipe, and $\mathrm{n}(\mathbf{x}) = 2$ inside a disk of radius 0.3 centered at $(0, 0.6)$. In order to keep the ratio of mesh size to wavelength roughly constant, the mesh inside the scatterer is refined according to the local refractive index. In Fig. 3 we show the spatial mesh and three snapshots of the same incident field as used in the previous section choosing the number of time steps $N_t = 512$ (from the previous

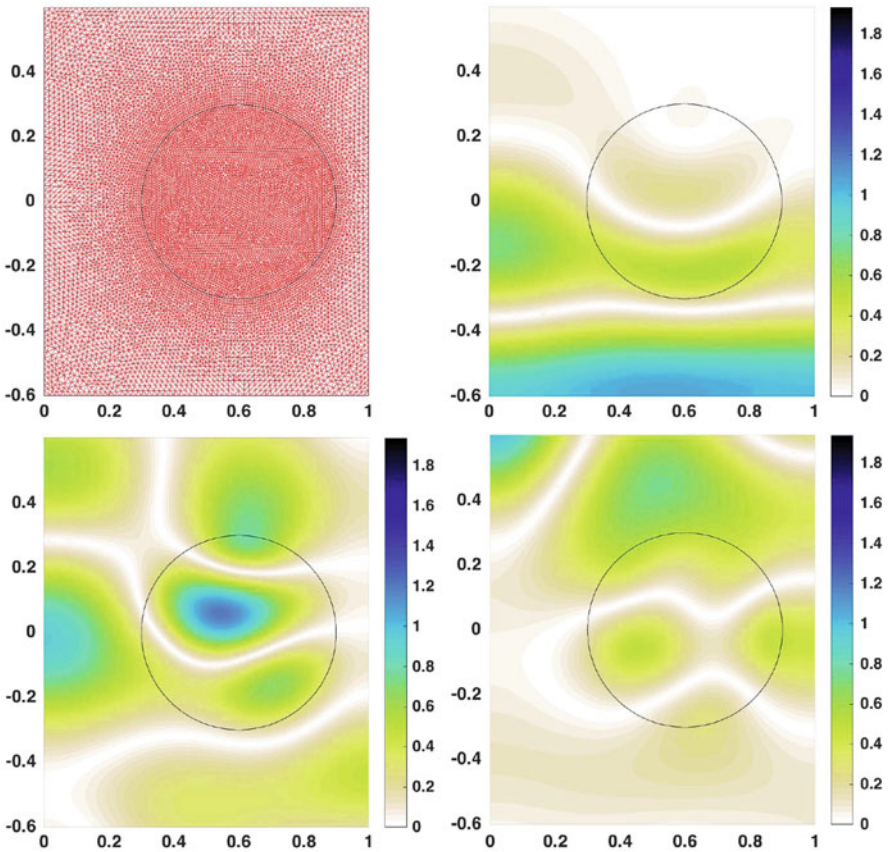

Fig. 3 Results for a penetrable scatterer. *Top left*: the spatial mesh, refined inside the scatterer. *Top right*: A snapshot of the total field at $t \approx 3$ when the incident wave is arriving at the scatterer from below. *Bottom left*: A snapshot of the total field at $t \approx 4$ when the maximum of the incident wave is at the scatterer. *Curved wave* fronts in the scatterer show that the wave has slowed there. *Bottom right*: A snapshot of the total field at $t \approx 5$ when the incident wave starts to pass the scatterer. A focal point is visible on the upper boundary of the scatterer

section we know the method propagates the incident wave with roughly 1% error when the obstacle is not present). Clearly, as expected, the waves slow down in the scatterer and are transmitted through the scatterer with a focal point on one side of the circle. No instability is evident.

In our second example we consider scattering from a sound soft obstacle. This corresponds to enforcing the Dirichlet boundary condition $u = 0$ on the boundary of the same disk as used in the previous example. Results are shown in Fig. 4.

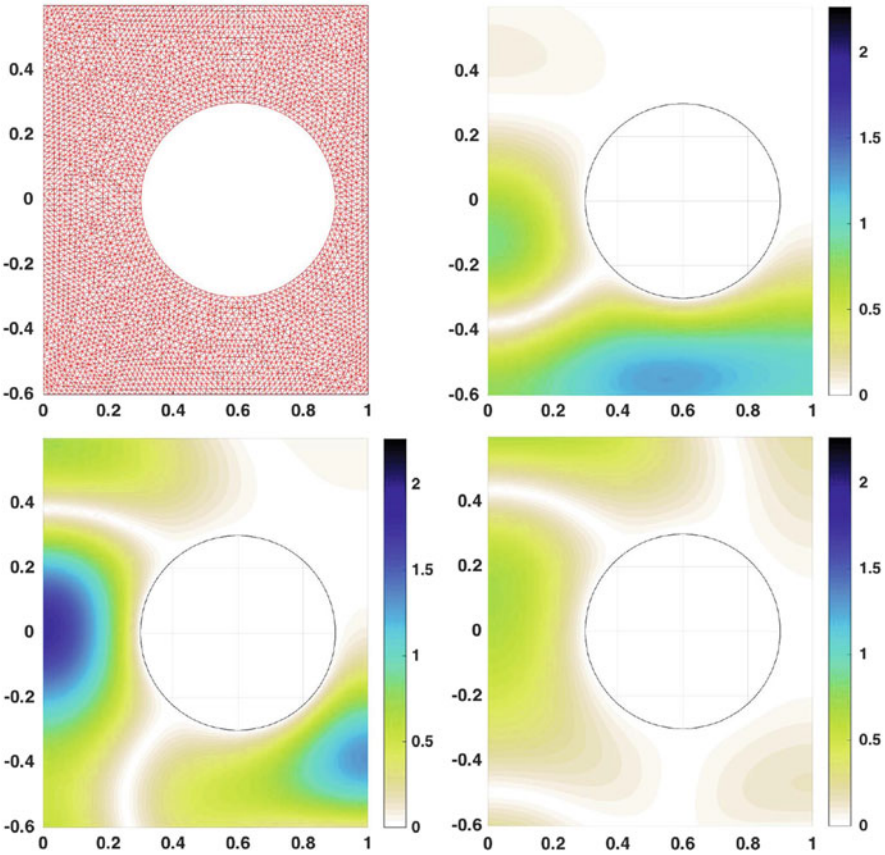

Fig. 4 Results for a sound soft scatterer. *Top left*: the spatial mesh. *Top right*: A snapshot of the total field at $t \approx 3$ when the incident wave is arriving at the scatterer from below. *Bottom left*: A snapshot of the total field at $t \approx 4$ when the maximum of the incident wave is at the scatterer. The incident wave is strongly reflected by the scatterer. *Bottom right*: A snapshot of the total field at $t \approx 5$ when the incident wave starts to pass the scatterer. Above the scatterer the wave is decreased in magnitude compared to Fig. 3 as is to be expected

5 Conclusions

In this paper we have shown how to derive and analyze a fully discrete time stepping method for the wave equation in an infinite pipe or waveguide. Using the DtN map to truncate the domain we obtain a coupled finite element and discrete DtN map for the discrete solution at each time step. Limited numerical results suggest the method is stable and accurate.

The main drawback of the method is that the solution needs to be recorded on the artificial boundaries to allow the convolution needed at each time step to be computed. However if there are only a few propagating modes in the solution this is not a crushing overhead unless very long solution times are required.

Acknowledgements The research of L. Fan and P. Monk was partially supported by NSF grant number DMS-1114889 and DMS-1125590. The research of V. Selgas by MTM2013-43671-P.

References

1. Bamberger, A., Duong, T.H.: Formulation variationnelle espace-temps pour le calcul par potentiel retarde de la diffraction d'une onde acoustique (I). Math. Meth. Appl. Sci. **8**, 405–435 (1986)
2. Banjai, L.: Time-domain Dirichlet-to-Neumann map and its discretization. IMA J. Numer. Anal. **34**, 1136–1155 (2014)
3. Banjai, L., Lubich, C., Sayas, F.: Stable numerical coupling of exterior and interior problems for the wave equation. Numer. Math. **129**(4), 611–646 (2015)
4. Banjai, L., Sauter, S.: Rapid solution of the wave equation in unbounded domains. SIAM J. Numer. Anal. **47**, 227–49 (2008)
5. Fan, L., Monk, P.: Time dependent scattering from a grating. J. Comput. Phys. **302**, 97–113 (2015)
6. Fan, L., Monk, P.: Time dependent scattering from a grating using convolution quadrature and the Dirichlet-to-Neumann map. (2015, submitted)
7. Ha-Duong, T.: On retarded potential boundary integral equations and their discretizations. In: Ainsworth, M., Davies, P., Duncan, D., Rynne, B., Martin, P. (eds.) Topics in Computational Wave Propagation: Direct and Inverse Problems, pp. 301–36. Springer, Berlin (2003)
8. Hecht, F.: New development in FreeFem++. J. Numer. Math. **20**, 251–265 (2012)
9. Lu, Y., Zhu, J.: Perfectly matched layer for acoustic waveguide modeling—benchmark calculations and perturbation analysis. Comput. Model. Eng. Sci. **22**, 235–248 (2007)
10. Lubich, C.: On the multistep time discretization of linear initial-boundary value problems and their boundary integral equations. Numer. Math. **67**, 365–89 (1994)